Volume 11 | Number 43 | 21 November 2015 | Pages 8385–8526

Soft Matter

www.softmatter.org

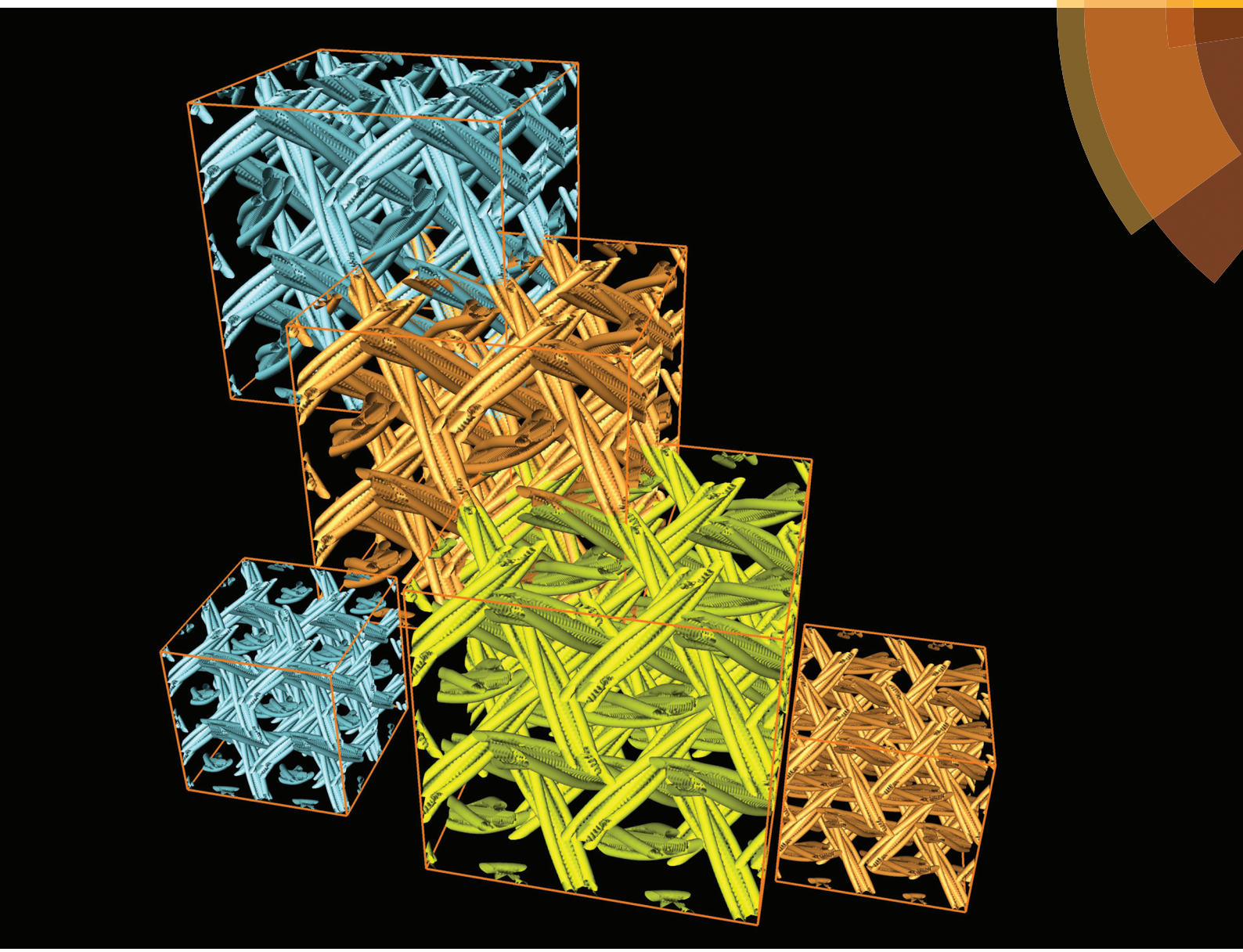

ISSN 1744-683X

ROYAL SOCIETY OF CHEMISTRY

PAPER
Miha Ravnik and Jun-ichi Fukuda
Templated blue phases

Soft Matter

PAPER

View Article Online
View Journal | View Issue

Open Access Article. Published on 17 September 2015. Downloaded on 12/10/2025 12:34:07 AM.
This article is licensed under a Creative Commons Attribution-NonCommercial 3.0 Unported Licence.

Cite this: *Soft Matter*, 2015, **11**, 8417

Templated blue phases

Miha Ravnik*[abc] and Jun-ichi Fukuda[b]

Received 28th July 2015,
Accepted 17th September 2015

DOI: 10.1039/c5sm01878a

www.rsc.org/softmatter

Cholesteric blue phases of a chiral liquid crystal are interesting examples of self-organised three-dimensional nanostructures formed by soft matter. Recently it was demonstrated that a polymer matrix introduced by photopolymerization inside a bulk blue phase not only stabilises the host blue phase significantly, but also serves as a template for blue phase ordering. We show with numerical modelling that the transfer of the orientational order of the blue phase to the surfaces of the polymer matrix, together with the resulting surface anchoring, can account for the templating behaviour of the polymer matrix inducing the blue phase ordering of an achiral nematic liquid crystal. Furthermore, tailoring the anchoring conditions of the polymer matrix surfaces can bring about orientational ordering different from those of bulk blue phases, including an intertwined complex of the polymer matrix and topological line defects of orientational order. Optical Kerr response of templated blue phases is explored, finding large Kerr constants in the range of $K = 2–10 \times 10^{-9}$ m V^{-2} and notable dependence on the surface anchoring strength. More generally, the presented numerical approach is aimed to clarify the role and actions of templating polymer matrices in complex chiral nematic fluids, and further to help design novel template-based materials from chiral liquid crystals.

1 Introduction

Soft materials including polymers, liquid crystals, colloids and amphiphiles are promising candidates for bottom-up nanotechnology because many of them self-assemble to form nanostructures with specific ordering and periodicity. One notable example is cholesteric blue phases (BPs) exhibited by liquid crystals with strong chirality.[1–3] Cholesteric BPs are three-dimensionally ordered phases comprising a complex network of topological line defects of orientational order (disclination lines), and orientational structures known as the double-twist cylinders in which twist distortions are present along all directions perpendicular to the cylinder axis. Three thermodynamically stable cholesteric BPs are known between the high-temperature isotropic phase and the low-temperature chiral nematic (or cholesteric) phase. Two BPs known as BP I and BP II possess cubic symmetry, whereas the third BP (BP III) is believed to be amorphous.[4] The lattice constant of cubic BPs is typically a few hundred nanometres, on the order of the wavelength of visible light. Owing to this periodic ordering, cholesteric BPs have attracted considerable interest as photonic materials; their photonic band structures were discussed theoretically,[5–7] and lasing in cholesteric BPs has been reported.[8,9]

Liquid crystals are important components of current display and beyond-the-display technology.[10] The relevance of blue phases as optical materials rose with the development of wide-temperature range blue phase materials, firstly in 2002 by introducing a photo-polymerised polymer matrix into blue phases,[11] and later in 2005 by developing blue phase bi-mesogenic materials.[12] Optical switching modes and photonic applications of blue phases are now being developed, including optical filters, optical attenuators, phase modulators, tunable lenses, and laser sources.[13–18] And in all these applications, the major approach for stabilising and realising optical and photonic elements from blue phases is by polymer/particle doping[19–21] and by photopolymerisation.[22,23]

Recently, it was demonstrated experimentally[24–26] that the polymer matrix introduced into a cholesteric BP could serve as a template for BP ordering of an achiral nematic liquid crystal that cannot exhibit cholesteric BPs by itself. Templated BPs of an achiral liquid crystal are advantageous over conventional BPs as they allow for use of already developed far more diverse and superior-property materials (*i.e.* chemical compounds), since the complex three-dimensional ordering of the phase is assured by the template matrix and not by the molecular details of the liquid crystalline fluid. For example, for blue phase display applications, high dielectric anisotropy and low viscosity materials are desirable as they assure low operating voltage and fast switching times, but it is not easy to design liquid crystals

[a] *Faculty of Mathematics and Physics, University of Ljubljana, Jadranska 19, 1000 Ljubljana, Slovenia. E-mail: miha.ravnik@fmf.uni-lj.si*
[b] *Research Institute for Sustainable Chemistry, National Institute of Advanced Industrial Science and Technology (AIST), 1-1-1 Higashi, Tsukuba 305-8565, Japan. E-mail: fukuda.jun-ichi@aist.go.jp*
[c] *Jozef Stefan Institute, Jamova 39, 1000 Ljubljana, Slovenia*

Open Access Article. Published on 17 September 2015. Downloaded on 12/10/2025 12:34:07 AM.
This article is licensed under a Creative Commons Attribution-NonCommercial 3.0 Unported Licence.

that meet these criteria and simultaneously exhibit BPs. And, templated blue phases of achiral nematics can easily achieve both. Therefore, understanding the response of BPs to doping is not only scientifically but also technologically important. A semi-quantitative analysis showed that the stabilisation of BPs could be accounted for by the replacement of energetically costly disclination core regions by a polymer matrix.[27] The templating behaviour strongly suggests that the BP ordering of the host liquid crystal is imposed by the surfaces of the polymer matrix *via* the surface anchoring mechanism. And the idea of this paper is to explore and demonstrate the role of different anchoring regimes that can be imposed by the polymer matrix on the host nematic fluid.

In this study, we explore the templated blue phases I and II infiltrated with an achiral nematic liquid crystal, considering three distinct (anchoring) regimes at the template matrix: (i) blue phase I or II surface memorised anchoring, (ii) homoeotropic (perpendicular) anchoring, and (iii) degenerate planar anchoring. By using numerical modelling based on the Landau-de Gennes free energy, we replace the liquid crystal regions with reduced orientational order – the defect lines – with the polymer matrix and explore how the surface anchoring imposed by the template matrices changes the orientational ordering of the nematic. We show that only sufficiently high surface anchoring interaction assures blue-phase-type orientational ordering, whereas weak surface anchoring results in homogeneous nematic-like profiles. We further demonstrate that matrix surfaces which impose homeotropic or degenerate planar anchoring give rise to intriguing disclination structures intertwined with the polymer matrix. The optic response of different templated blue phases is investigated by considering the electro-optic Kerr effect, where different regimes of macroscopic optical isotropy and anisotropy are observed. Characteristic Kerr constants are calculated, showing that they strongly depend on the type and strength of the surface anchoring of the template matrix.

2 Modelling and theory

Templated blue phases are distinct for their mesoscopic variation of molecular order, and a strong approach for modelling of such materials is by a phenomenological free energy minimisation technique.[28–30] The local molecular order is described by nematic order parameter tensor Q_{ij}, which encompasses the general (chiral and achiral) orientational ordering of nematic molecules and the formation of topological defects, both central in the blue phase-based liquid crystalline materials. Tensorial invariants of Q_{ij} are used to construct the bulk free energy density of a chiral (blue phase) nematic fluid f_B:

$$f_B = \frac{A_0(1-\gamma/3)}{2}Q_{ij}Q_{ji} - \frac{A_0\gamma}{3}Q_{ij}Q_{jk}Q_{ki} + \frac{A_0\gamma}{4}(Q_{ij}Q_{ji})^2 + \frac{L}{2}\frac{\partial Q_{ij}}{\partial x_k}\frac{\partial Q_{ij}}{\partial x_k} + 2q_0L\varepsilon_{ikl}Q_{ij}\frac{\partial Q_{lj}}{\partial x_k}, \quad (1)$$

where A_0 is the material parameter characterising the nematic degree of order S, γ is the effective temperature, L is the single nematic elastic constant, ε_{ikl} is the Levi-Civita totally asymmetric tensor, and $q_0 = 2\pi/p_0$ is the inverse pitch that determines the periodicity of the characteristic helical ordering in the cholesteric phase and is related to the unit cell size of the cubic blue phases. Notably, the last term in eqn (1) imposes and stabilises the chiral ordering in blue phases; therefore, by setting $q_0 = 0$, the chiral ordering can be changed into a regular uniaxial achiral nematic. Indeed, in the considered templated blue phases, the complex blue phase-like molecular orientational order will be imposed by the surfaces of the template (*e.g.* polymer) matrix rather than by the bulk chirality of the material.

The templated blue phases are a hybrid material where both the template matrix and the nematic orientational profile need to be considered. We approach their structure by using a two stage calculation. In Stage 1, we first calculate the full equilibrium orientational profile of the bulk blue phase I or II (with no template) and then identify the blue phase defect regions as corresponding to the polymer template. The cut-off interface of the template is set by the isosurface of constant nematic degree of order (S_{cutoff}) – see red regions in Fig. 1a and b. Such an allocation of the template can be justified in the view of recent experiments, where the polymers get attracted exactly into the defect regions to minimise the distorted volume of the chiral nematic, eventually forming the template.[24,25,27] In Stage 2, the surface anchoring is implemented at the surface of the template, and the surrounding fluid is set as a regular (non-chiral) nematic by taking $q_0 = 0$. Under these new boundary conditions, now imposed by the template matrix, and taking non-chiral nematic, the nematic Q tensor profile is again equilibrated.

The template matrix can impose two types of molecular alignment (anchoring) at the surface: (i) uniform alignment along one distinct direction such as perpendicular to the surface (homeotropic) or along the surface, and (ii) degenerate alignment within the surface plane. The anchoring is described by introducing uniform and degenerate surface free energy density at the matrix surface, $f_S^{uni} = W_{uni}(Q_{ij} - Q_{ij}^0)^2/2$ and $f_S^{deg} = W_{deg}(\tilde{Q}_{ij} - \tilde{Q}_{ij}^{\perp})^2$, respectively. Here, Q_{ij}^0 is the surface imposed nematic order parameter tensor and projected tensors $\tilde{Q}_{ij}$ and $\tilde{Q}_{ij}^{\perp}$ are defined according to ref. 31 and 32. In the following, three distinct surface alignment regimes will be considered, as most relevant for typical experimental regimes: (i) uniform inplane anchoring with memorised blue phase director pattern, (ii) uniform homeotropic anchoring and (iii) degenerate planar anchoring. For the uniform inplane anchoring with memorised blue phase, we take the director of the non-templated blue phase (as calculated in Stage 1 of the calculation) and use it as the easy-direction of the uniform anchoring implemented through the anchoring tensor Q_{ij}^0. Actually, it is exactly this blue phase memorised uniform inplane anchoring which seems the most desirable in the view of applications of the templated blue phases, as it effectively fully retains the optical properties of un-templated blue phases. Finally, more generally, it is important to notice that the three anchoring regimes correspond to three very different templated blue phase materials, each with different mesophase and optical properties.

The optical response of the templated blue phases to an external electric field – the Kerr effect – is determined by calculating the

 This journal is © The Royal Society of Chemistry 2015

Open Access Article. Published on 17 September 2015. Downloaded on 12/10/2025 12:34:07 AM.
This article is licensed under a Creative Commons Attribution-NonCommercial 3.0 Unported Licence.

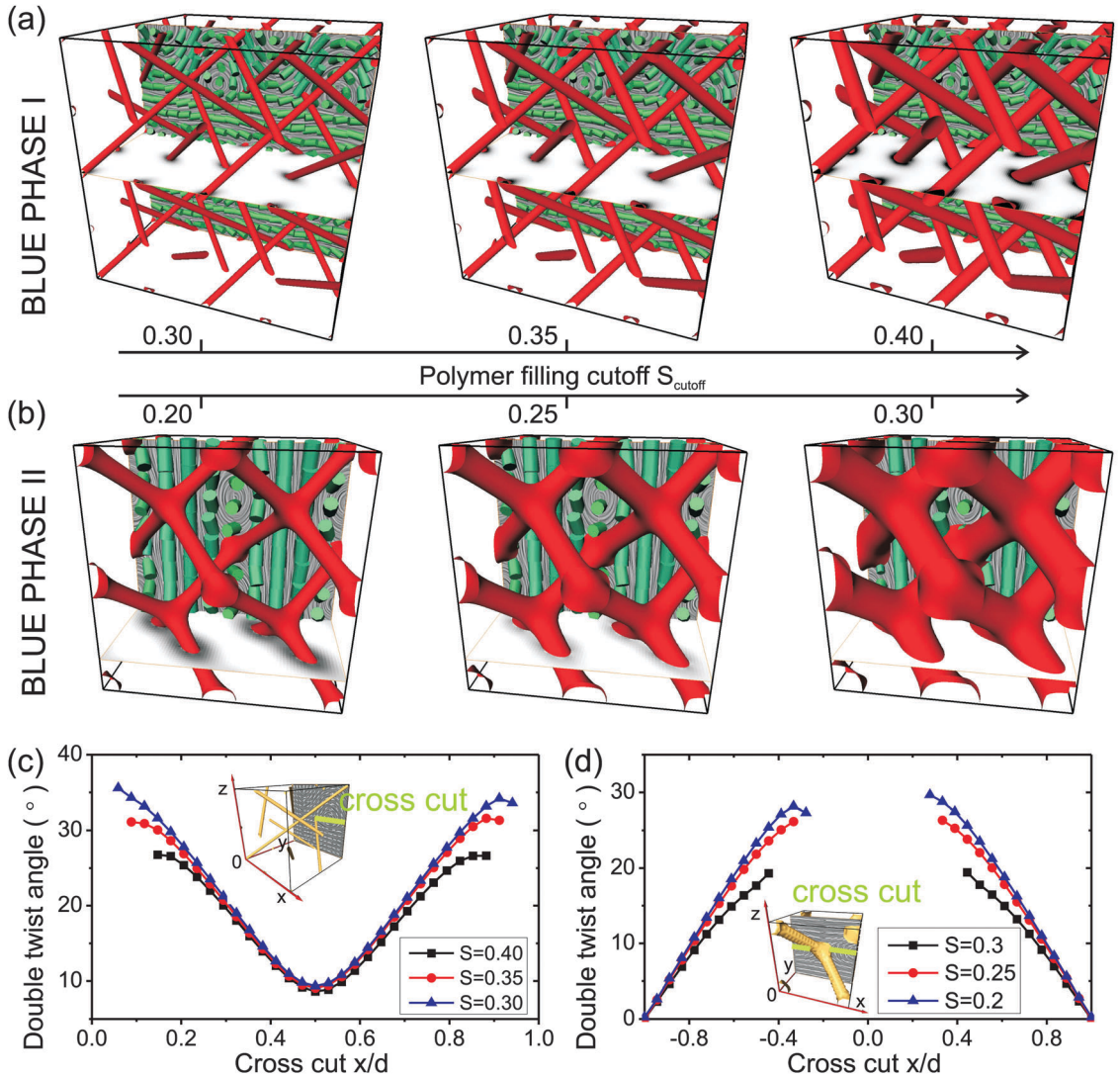

Fig. 1 Templated blue phases I and II of achiral nematic with with blue phase memorised surface anchoring. A polymer template for various polymer filling cut-offs (in red) and the corresponding director profile (in green) and variable nematic degree of order (in grayscale; horizontal plane) for nematic templated (a) blue phase I and (b) blue phase II. A double twist director angle across a double twist cylinder (see insets) for nematic templated (c) blue phase I and (d) blue phase II. Cross-cut in (c) is along the line from point ($a_{BPI}/2$, a_{BPI}, $a_{BPI}/2$) to (a_{BPI}, a_{BPI}, $a_{BPI}/2$) and in (d) from (0, $a_{BPII}/2$, $a_{BPII}/2$) to (a_{BPII}, $a_{BPII}/2$, $a_{BPII}/2$), according to the Cartesian coordinates indicated in the inset. Strong surface anchoring is assumed to be (W_{uni} = 10^{-3} J m^{-2}).

Kerr constant K.[33,34] The coupling between the nematic orientational profile and the external electric field E_i is incorporated *via* the dielectric free energy volume density $f_{diel} = -\varepsilon_0 \varepsilon_a^{mic} E_i Q_{ij} E_j/3$, where ε_a^{mic} is the low-frequency microscopic nematic dielectric anisotropy. Effectively, the Kerr constant measures the emergent macroscopic birefringence Δn of the material and characterises the average optical response of typically multiple blue phase cells (Δn is not (!) the difference between the ordinary and extraordinary refractive index). In the Kerr effect, the birefringence is proportional to the square of the electric field E, as:

$$\Delta n = \lambda K E^2 \qquad (2)$$

where λ is the wavelength of light. We calculate the Kerr constant by averaging the dielectric permittivity tensor at optical frequencies over the unit cell of the templated blue phase also using the calculated nematic order parameter tensor as:

$$\bar{\varepsilon}_{ij} = \frac{1}{V}\int\left(\bar{\varepsilon}\delta_{ij} + \frac{2}{3}\varepsilon_a^{mol} Q_{ij}\right) dV, \qquad (3)$$

where $\bar{\varepsilon}$ is the average dielectric permittivity, $\varepsilon_a^{mol} = \varepsilon_{\parallel}^{mol} - \varepsilon_{\perp}^{mol}$ is the molecular dielectric anisotropy at optical frequencies, and the integration is performed over the whole volume V of the unit cell of the templated blue phase. The average dielectric permittivity tensor $\bar{\varepsilon}_{ij}$ is then diagonalised, and the difference between the (square-rooted) eigenvalues corresponds to the macroscopic birefringence Δn. Notably, we should comment that for some specific BP templated structures under the electric field (with homeotropic and planar degenerate anchoring) we observe also

Open Access Article. Published on 17 September 2015. Downloaded on 12/10/2025 12:34:07 AM.
This article is licensed under a Creative Commons Attribution-NonCommercial 3.0 Unported Licence.

that all three eigenvalues of the average permittivity tensor become nondegenerate, indicating biaxial optical response rather than the uniaxial Kerr effect. Also, we should comment that Pockels effect was observed in some templated blue phase systems, *i.e.* linear dependence of induced birefringence on external electric field.[23]

The following numerical parameters are used in calculations. In Stage 1, to generate the blue phase template matrices, we use single elastic constant $L = 2.5 \times 10^{-11}$ N, nematic bulk material parameter $A_0 = 1.02 \times 10^{-5}$ J m^{-3}, and ($p_0 = 0.651$ μm, $\gamma = 3.857$) for BP I and ($p_0 = 0.590$ μm, $\gamma = 3$) for BP II, which corresponds to equilibrium unit cell size of $a_{\mathrm{BPI}} = 680$ nm for BP I and $a_{\mathrm{BPII}} = 360$ nm for BP II. These values are kept the same in all calculations. In Stage 2, to calculate the orientational profile of (achiral) nematic templated blue phases, we use single elastic constant $L = 2.5 \times 10^{-11}$ N, nematic bulk material parameter $A_0 = 1.02 \times 10^{-5}$ J m^{-3}, $q_0 = 0$, and $\gamma = 3.857$ for templated BP I and $\gamma = 3$ for templated BP II. For Kerr constant calculations, the electric field is applied along the vertical principal unit cell direction (*i.e.* along the edge of the unit cell, z direction) and material parameters $\varepsilon_{\mathrm{a}}^{\mathrm{mic}} = 10$, $\bar{\varepsilon} = 2.46$, and $\varepsilon_{\mathrm{a}}^{\mathrm{mol}} = 1.07$ are used. The parameter values are chosen to correspond to typical values of an achiral nematic such as 5CB and the typical value of cubic blue phases I and II.

3 Results

3.1 Templated blue phases with blue phase memorised surface anchoring

The two main variabilities of templated blue phases are their polymer filling fraction and the polymer matrix-to-liquid crystal interaction, *i.e.* the surface anchoring at the matrix surface. Fig. 1 and 2 show the (nonchiral) nematic profiles stabilised by the memorised anchoring of BP I and BP II at the polymer matrix surfaces. In both nematic templated blue phase I and blue phase II, the three-dimensional profile of (achiral) nematic almost perfectly reproduces the three-dimensional orientational director pattern of (chiral) blue phases with no template. For example, in Fig. 1a and b, one can clearly find the well known stacks of double-twist cylinders characteristic for blue phases, but now importantly formed by achiral nematic under the confinement of the polymer matrix. The exact polymer filling cut-off value – effectively, the thickness of the templated network – is also observed to have only a small effect on the actual director profile of the double twist cylinders which roughly remain of the same profile (Fig. 1c and d).

The nematic profile within templated blue phases with blue phase memorised surface anchoring exhibits two distinct ordering regimes (*i.e.* two ordering states) depending on the polymer filling cut-off and the anchoring strength at the nematic-to-polymer–matrix interface, as shown in Fig. 2. At higher anchoring strengths, the BP-like profiles are imposed by the memorised surface anchoring. However, if the anchoring is rather weak, the nematic ignores the template surface imposed pattern and aligns into a homogeneous director state with regions of reduced degrees of order close to surfaces with conflicting alignment. Such confinement-induced transitions into a homogeneous director state are well known, *e.g.* from nematic droplets[35] where bulk nematic elasticity (scales as $\propto R$,

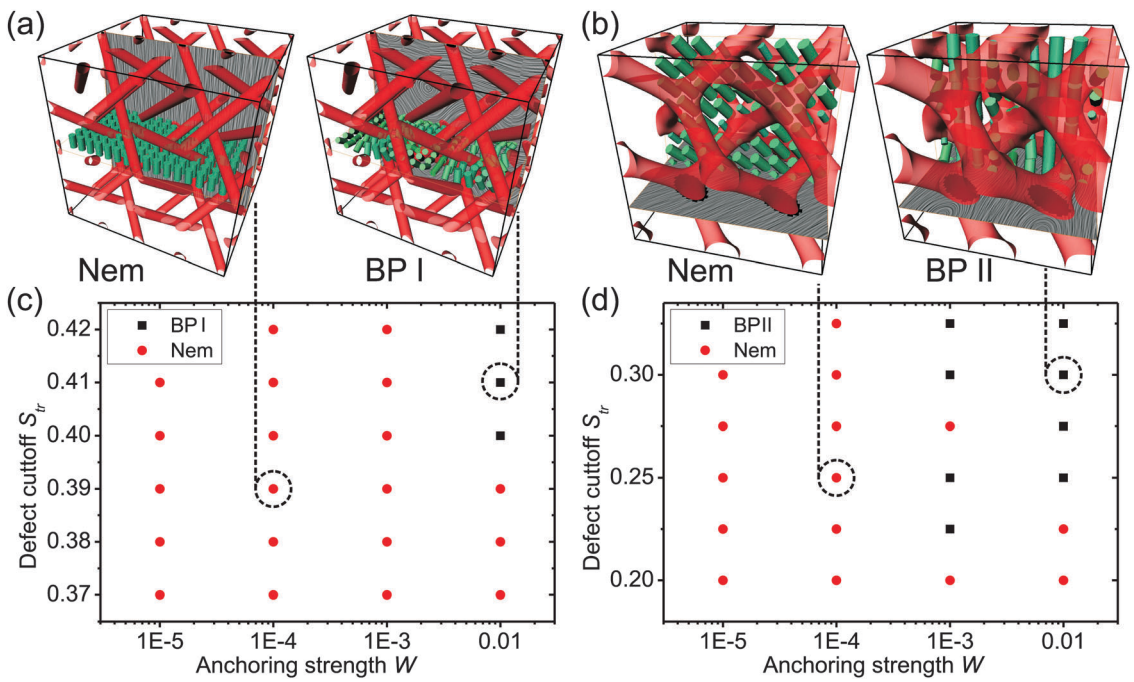

Fig. 2 Phase diagram of achiral nematic templated (a and c) blue phase I and (b and d) blue phase II with blue phase memorised surface anchoring. A homogeneous nematic profile (Nem) or a surface stabilised blue phase-like pattern is observed depending on the template surface anchoring strength or the defect cut-off (*i.e.* polymer filling fraction). In (a) and (b), red shows the template matrix, green cylinders visualise the director in a given plane, and grey stripes show the projection of the director onto the given plane.

 This journal is © The Royal Society of Chemistry 2015

Open Access Article. Published on 17 September 2015. Downloaded on 12/10/2025 12:34:07 AM.
This article is licensed under a Creative Commons Attribution-NonCommercial 3.0 Unported Licence.

where R is the droplet size) overcomes the surface anchoring effects (scale as $\propto R^2$) in small droplets ($R \to 0$).

3.2 Templated blue phases with homeotropic surface anchoring

Nematic templated blue phases with homeotropic (perpendicular) surface anchoring at the nematic-to-template interface are explored as an idea to achieve novel optical response from the same templated material, changing only the functionalisation of the surface. The actual realisation of homeotropic anchoring at the interface between the template matrix and nematic could possibly be achieved by smart material design, including (i) the choice of material used to form the matrix, such as the type of polymer, (ii) the liquid crystal used to infiltrate the matrix, and (iii) the addition of material-compatible surfactants that impose homeotropic anchoring. Some of the above-mentioned approaches are reported in ref. 36–38.

Fig. 3 shows nematic profiles formed within the homeotropic template of blue phase I (Fig. 3a–d) and of blue phase II (Fig. 3e–g). Notably, in templated blue phase I, at higher anchoring strengths, we observe a bistability of two patterns (Fig. 3a and b). The first pattern is reminiscent of the blue-phase director profile (Fig. 3a and b, left panel), whereas the second corresponds to a homogeneously aligned nematic perturbed with the presence of the template (Fig. 3a and b, right panel). The characteristic fingerprint of these two patterns is a trio – for blue phase-like – or a pair – for nematic-like – of $-1/2$ disclination lines which encircle the template network.

In templated blue phase II, we also see the formation of two distinct nematic profiles: (i) profile with bulk point defects

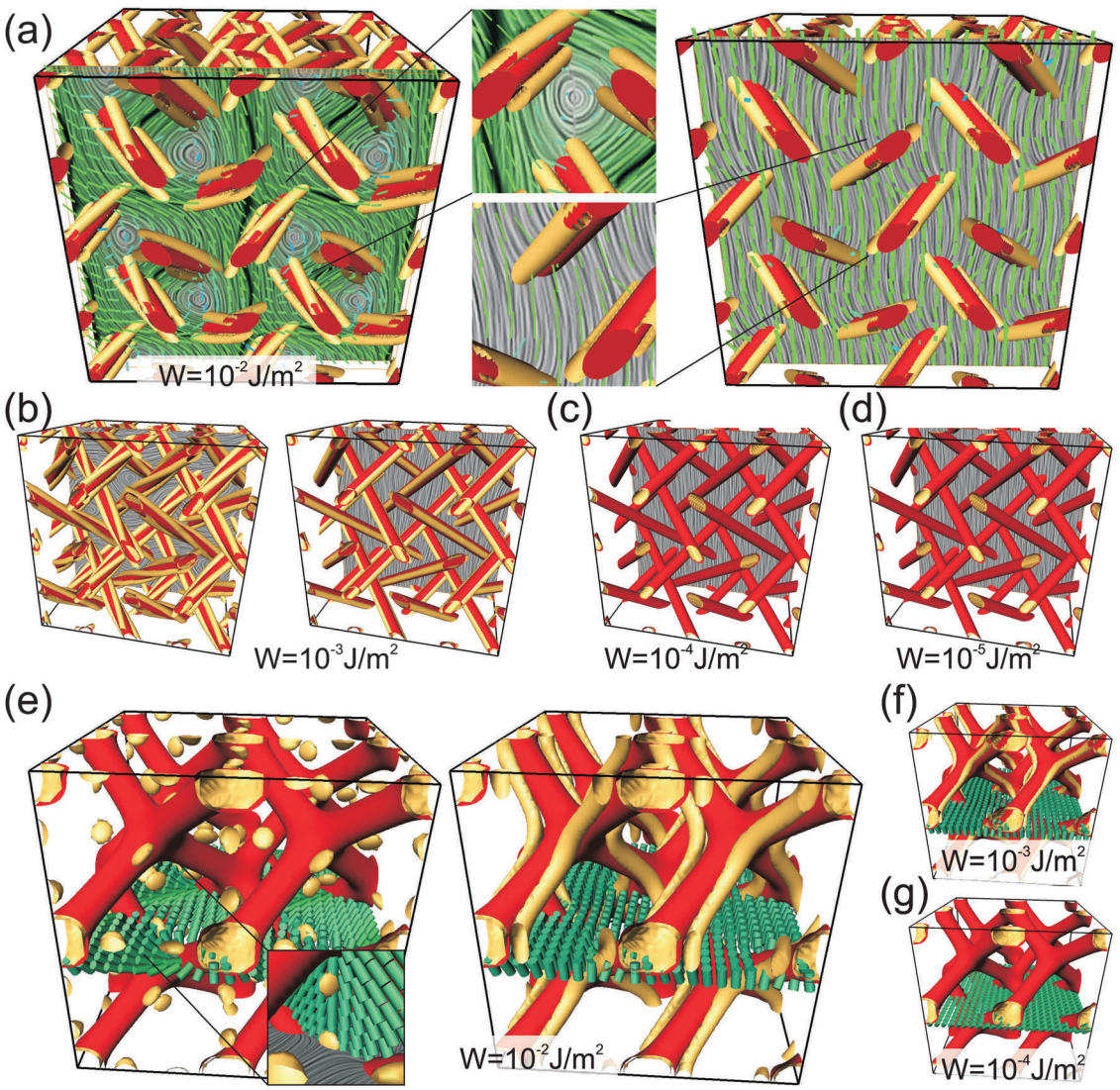

Fig. 3 Templated blue phases with homeotropic surface anchoring. (a) Three-disclination profile (left) and two-disclination profile (right) of templated blue phase I at strong surface anchoring regime. The insets show details of the nematic director in selected planes. (b–d) Templated blue phase I profiles at different anchoring strengths W. (e–g) Profiles of templated blue phase II for different anchoring strengths. The template matrix (in red) is selected at $S_{cutoff} = 0.4$ for BP I and $S_{cutoff} = 0.25$ for BP II. Nematic defects are drawn (in yellow) as isosurfaces of nematic degree of order $S = 0.34$ (BP I) and $S = 0.19$ (BP II). The director is visualised by green cylinders in selected planes and director projection to a given plane is drawn by grey streamlines.

Open Access Article. Published on 17 September 2015. Downloaded on 12/10/2025 12:34:07 AM.
This article is licensed under a Creative Commons Attribution-NonCommercial 3.0 Unported Licence.

(Fig. 3e, left panel) and (ii) structure with a pair of defect lines following the template (Fig. 3e, left panel). Their emergence and (meta)stability is strongly dependent on the anchoring strength. The profile with point defects is characterised by strong 3D variation of the nematic director, whereas the profile with a pair of disclinations exhibits an aligned (homogeneous-like) director which is perturbed by the template surface. The rough aligning direction is observed to typically coincide with the symmetry directions of the template matrix (*e.g.* see Fig. 3e), *i.e.* such as along the edge of the unit cell cube.

The distinct number of defect lines compensating for the homeotropic profiles imposed by the blue phase I and blue phase II templates is conditioned by the topology of the general nematic field (reminiscent of far-field). As the general topology of three-dimensional nematic fields of blue phase-like pattern is difficult to determine because of unclosed defect networks, simple observations based on the winding number invariant in distinct geometrical cross-sections (*i.e.* planes) can be made (for more on topology of nematics, please see ref. 39). For the nematic-like profile, the director is topologically equivalent to a homogeneous far field; thus locally two winding number −1/2 disclinations are needed to compensate for the surface-imposed pattern which is equivalent to a +1 disclination. Differently, in the regimes with three −1/2 disclinations, the defect lines compensate not only for the distortion imposed by the template (of +1 winding number) but effectively, also the profile imposed by the double twist cylinders, which – although not having a singular director – are equivalent to +1 defect lines.

3.3 Templated blue phases with degenerate planar surface anchoring

As the third experimentally relevant surface functionalisation we consider templated blue phases with planar degenerate surface anchoring. Again, similarly as for homeotropic templated blue phases, such inplane anchoring could emerge or be created by smart selection of LC, matrix materials, and surfactants.

Nematic profiles of templated blue phases with degenerate planar anchoring are shown in Fig. 4. For the blue phase I template, we observe a trio or a pair of surface defect lines (Fig. 4a left and right, respectively), which topologically, are generalisation of boojum defects. In order to compensate for the director variation imposed by the double twist cylinders, the relative angle of the surface defect trio is rotated by an angle of 60° and for the pair of defect lines by an angle of 90° as compared to the defect positions of the bulk disclinations in homeotropic templated blue phases (Fig. 3). For the blue phase II template with planar anchoring (Fig. 4b–d), a roughly homogeneous nematic profile is observed which is perturbed by the surface. Notably, for the blue phase II template, the general director direction within the unit cell is always aligned along one of the template arms (*i.e.* along the body diagonal of the unit cell cube, see green cylinders in Fig. 4b) in order to minimise the nematic distortion.

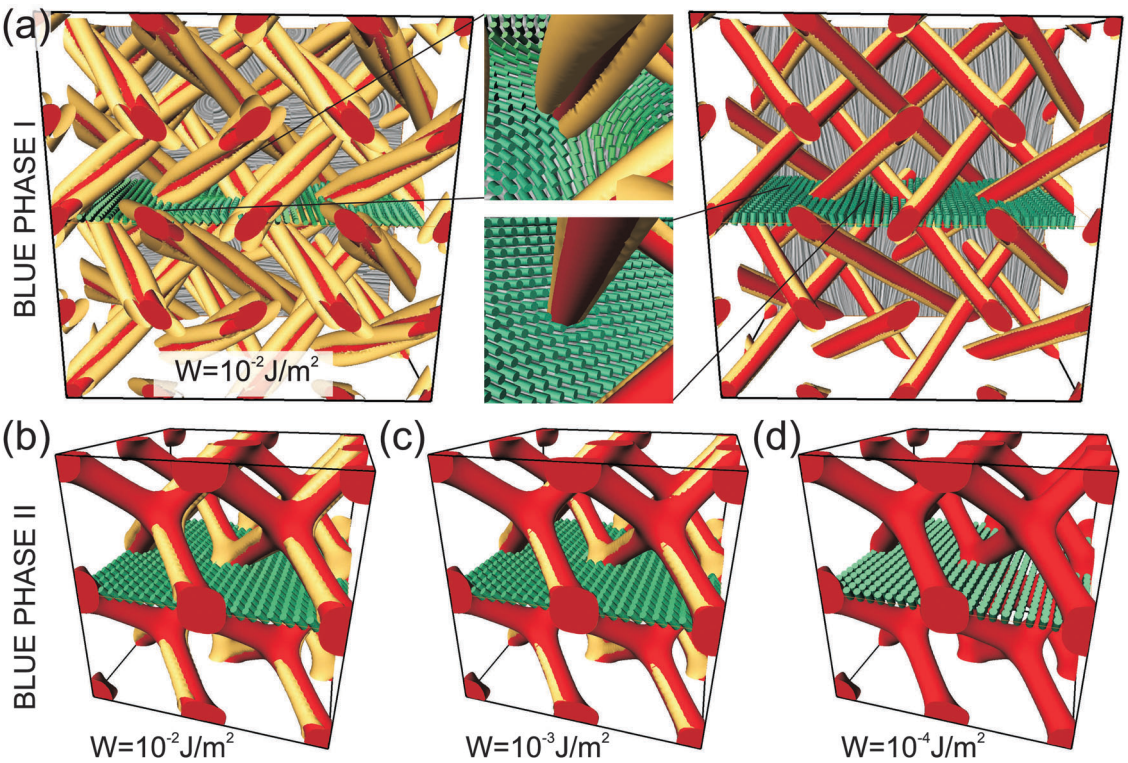

Fig. 4 Templated blue phases with degenerate planar surface anchoring. (a) Three-surface defect line profile (left) and two-surface defect line profile are observed for templated blue phase I. The insets show the nematic director (green cylinders) in selected planes. (b–d) Templated blue phase II profiles for different anchoring strengths W. The template matrix (in red) is selected at S_{cutoff} = 0.4 (BP I) and at S_{cutoff} = 0.25 (BP II). Nematic defects are drawn as isosurfaces of nematic degree of order S = 0.37 (BP I) and S = 0.16 (BP II). The director is visualised by green cylinders in selected planes and director projection to a given plane is drawn by grey streamlines.

 This journal is © The Royal Society of Chemistry 2015

Open Access Article. Published on 17 September 2015. Downloaded on 12/10/2025 12:34:07 AM.
This article is licensed under a Creative Commons Attribution-NonCommercial 3.0 Unported Licence.

Namely, such a director orientation allows for the template arms which are parallel to the director to be free of surface defects.

3.4 Kerr effect of templated blue phases

A major interest in blue phases is for their application as optical materials, in particular as materials with a large Kerr effect.[40,41] Therefore, the presented templated blue phases are analysed in the view of their Kerr response, *i.e.* we calculate their induced birefringence Δn upon applying an external electric field. The homogeneous electric field is applied along the direction of the vertical edge of the cubic unit cell (z direction, see Fig. 5).

Fig. 5 shows the Kerr response of templated blue phases for all three types of their surface anchoring: (i) blue phase memorised surface anchoring (Section 3.1), (ii) homeotropic anchoring (Section 3.2), and (iii) degenerate planar anchoring (Section 3.3). For templated blue phase I (Fig. 5), linear dependence of induced birefringence Δn on the square of electric field (E^2) is observed, indicating the Kerr behaviour. The following Kerr constants (for the wavelength of light λ = 500 nm) are extracted: $K_{\mathrm{BPI}} = 2.28 \times 10^{-9}$ m V^{-2}, $K_{\mathrm{BPI\,Hom}} = 4.08 \times 10^{-9}$ m V^{-2} and $K_{\mathrm{BPI\,Plan}} = 10.98 \times 10^{-9}$ m V^{-2}. These values are notably larger as compared to the Kerr constant of templated blue phase I with memorised blue phase I anchoring and infiltrated with chiral nematic $K_{\mathrm{BPI\,chiral}} = 1.38 \times 10^{-9}$ m V^{-2} (green dashed line in Fig. 5a), indicating that the effectively larger rigidity of chiral nematic allows only for relatively weaker optical response upon the applied external field. For templated blue phase II, the calculations of the effective (induced) birefringence reveal that both the two stable homeotropic- and planar-anchoring structures (see bottom panels in Fig. 5) are optically anisotropic, even at the zero external electric field. This inherent effective macroscopic optical anisotropy (averaged over the whole unit cell) originates from the actual structure of the nematic profile. In contrast, the templated profile with blue phase II memorised surface profile gives clear Kerr response with a Kerr constant of $K_{\mathrm{BPII}} = 2.02 \times 10^{-9}$ m V^{-2}. The Kerr constant of the templated blue phase II with blue phase II memorised surface profile and infiltrated with chiral nematic is calculated to be $K_{\mathrm{BPII}} = 0.707 \times 10^{-9}$ m V^{-2} (slope of the green dashed line shown in Fig. 5b), again indicating that chiral nematic gives weaker optical response compared to achiral nematic when infiltrating templated blue phases. The calculated values of Kerr constants are in the range of the Kerr constants of non-templated standard blue phases – but interestingly somewhat larger. For example, Kerr constants of $K = 3.7 \times 10^{-10}$ m V^{-2} [40] and $K = 5 \times 10^{-10}$ m V^{-2} [42] are reported in the literature for polymer stabilised blue phases, and $K = 10$–100×10^{-10} m V^{-2} [42] for amorphous blue phases.[33] Our calculated results – *i.e.* the largest Kerr response for planar degenerate anchoring – could be interpreted from the perspective that planar degenerate anchoring allows for freedom in director rotations than memorised anchoring and homeotropic anchoring, which results in a larger Kerr constant in the BP I case, and larger spontaneous birefringence in the BP II case.

The optical response of templated blue phases is observed to also notably depend on the strength of the surface anchoring. Selected results are given in Table 1, where the surface

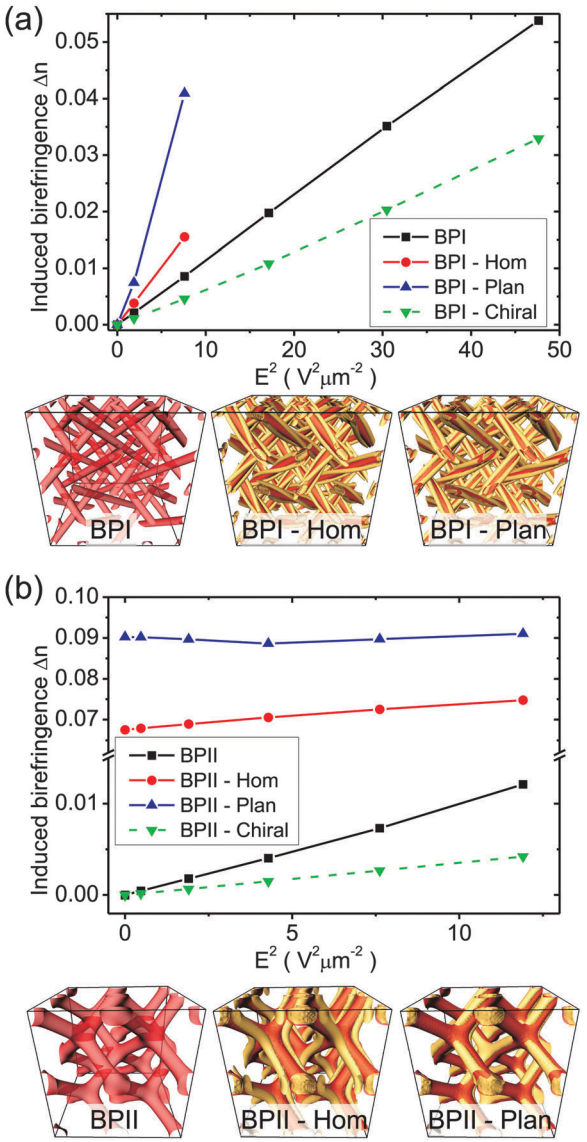

Fig. 5 Kerr response of templated blue phases with: memorised blue phase surface anchoring, homeotropic surface anchoring, and planar degenerate anchoring. (a) Induced birefringence for different structures of templated blue phase I. (b) Induced birefringence of templated blue phase II. For electric fields larger than presented, the structures become unstable. Structures with the same template cut-off value are compared: S_{cutoff} = 0.40 for BP I and S_{cutoff} = 0.25 for BP II. An electric field was applied along the vertical (z) direction. To allow comparison, in (a) and (b), we also show induced birefringence calculated for templated blue phases with memorised blue phase surface anchoring filled with chiral nematic with pitch p_0 = 0.651 μm for BP I and p_0 = 0.590 μm for BP II templates (in green, dashed lines).

anchoring strength W at the interface between the nematic and the template matrix is varied. As a general trend, we find that – if the selected blue phase pattern remains (meta)stable and does not decay into another lower free-energy structure when changing the anchoring (*e.g.* see phase diagrams in Fig. 2) – by decreasing the surface anchoring strength the Kerr constant increases. For example, in templated blue phase I with homeotropic anchoring, reducing the anchoring strength from

Open Access Article. Published on 17 September 2015. Downloaded on 12/10/2025 12:34:07 AM.
This article is licensed under a Creative Commons Attribution-NonCommercial 3.0 Unported Licence.

Table 1 Variation of the Kerr constant upon changing the surface anchoring strength W. Kerr constants are reported for four regimes of templated blue phases: (BP I Hom) templated blue phase I with homeotropic surface anchoring, (BP I Chiral) templated blue phase I with memorised blue phase I surface anchoring and infiltrated with chiral nematic, (BP II) templated blue phase II with memorised blue phase II surface anchoring, and (BP II Chiral) templated blue phase II with memorised blue phase II anchoring and infiltrated with chiral nematic

Templated blue phase	Anchoring strength (J m^{-2})	Kerr constant K (10^{-9} m V^{-2})
BP I Hom	0.01	4.08
	0.001	5.08
BP I Chiral	0.01	1.38
	0.001	1.73
	0.0001	2.58
BP II	0.01	2.02
	0.001	3.42
BP II Chiral	0.01	0.71
	0.001	0.92
	0.0001	1.35

$W = 0.01$ J m^{-2} to $W = 0.001$ J m^{-2} increases the Kerr constant by 20%. Similarly, in templated blue phase II with memorised blue phase II anchoring, the change in the anchoring strength from $W = 0.01$ J m^{-2} to $W = 0.001$ J m^{-2} increases the Kerr constant by 70%. In templated blue phases infiltrated with chiral nematic, even larger range of variability in the Kerr constants can be achieved *via* tuning the anchoring (see Table 1, BP I Chiral and BP II Chiral) because the structures are stable over a larger range of anchoring strengths. Qualitatively, the observed trend of increasing Kerr constants by reducing anchoring – under conditions that the blue phase patterns remain stable and do not transform into another pattern – could be explained by noticing that weaker anchoring effectively allows for stronger reorientations of the nematic – also close to the template surface. Therefore, when exposed to a given external electric field, larger optical response can emerge and in turn a larger Kerr constant.

Finally, more broadly, we have demonstrated the possibility of enhancing the Kerr effect by modifying and optimising the type and strength of the surface anchoring as imposed by the templating polymer matrix.

4 Conclusion

In conclusion, templated nematic-filled cubic blue phases I and II with different surface functionalisation – blue phase memorised, homeotropic and degenerate planar – are explored, finding multiple optically different and distinct structures. For blue phase memorised surfaces, the nematic profiles emerge strongly similar to profiles of bulk (non-templated) blue phases. For homeotropic surfaces, structures with trios or pairs of bulk defect lines emerge. And for degenerate planar surfaces, surface defect lines are observed, which are topological generalisations of surface boojum defects. The stability and metastability of the structures are shown to be strongly dependent on the anchoring strength at the template–nematic interface. From a more broad perspective, the observed profiles are also interesting examples of complex topology, such as the coupled disconnected periodic surface and bulk defect patterns that could be used to explore the general properties of topology of fields.

The different templated blue phases are shown to work as diverse optical Kerr materials, with Kerr constants of large typical values of $K = 2\text{–}10 \times 10^{-9}$ m V^{-2} for wavelength of light $\lambda = 500$ nm. The Kerr constants of selected blue phase profiles – if remaining (meta)stable – are shown to increase by decreasing the surface anchoring at the template–nematic interface. Selected profiles are also shown to inherently attain effective macroscopic optical anisotropy, the characteristic very different from typically expected blue phase-originating materials (that are macroscopically optically isotropic). More broadly, this work is motivated by designing novel optical anisotropy-based materials, and clearly already a simple variability in surface functionalisation of templated blue phases is shown to open a new route to novel fascinating optical soft materials.

Acknowledgements

The authors thank the Japan Society for the Promotion of Science (JSPS) whose Invitation Fellowship Program enabled M.R. to stay at National Institute of Advanced Industrial Science and Technology (AIST) and to initiate this work. J.F. is supported by JSPS Grant-in-Aid (KAKENHI) for Scientific Research (C) (Grant No. 25400437), and the Cooperative Research Program of "Network Joint Research Center for Materials and Devices". M.R. also acknowledges funding from Slovenian Research Agency Programme P1-0099, research project Z1-5441 and EU FP7 MC CIG grant FREEFLUID.

References

1 D. C. Wright and N. D. Mermin, *Rev. Mod. Phys.*, 1989, **61**, 385.
2 P. P. Crooker, in *Chirality in liquid crystals*, ed. H.-S. Kitzerow and C. Bahr, Springer, Berlin, 2001, ch. 7.
3 H. Kikuchi, *Struct. Bonding*, 2008, **128**, 99.
4 O. Henrich, K. Stratford, M. E. Cates and D. Marenduzzo, *Phys. Rev. Lett.*, 2011, **106**, 107801.
5 R. M. Hornreich, S. Shtrikman and C. Sommers, *Phys. Rev. E: Stat. Phys., Plasmas, Fluids, Relat. Interdiscip. Top.*, 1993, **47**, 2067.
6 Y. Ogawa, J. Fukuda, H. Yoshida, A. Fujii and M. Ozaki, *Opt. Lett.*, 2013, **38**, 3380; Y. Ogawa, J. Fukuda, H. Yoshida and M. Ozaki, *Opt. Express*, 2014, **22**, 3766.
7 M. Stimulak and M. Ravnik, *Soft Matter*, 2014, **10**, 6339.
8 W. Cao, A. Muñoz, P. Palffy-Muhoray and B. Taheri, *Nat. Mater.*, 2002, **1**, 111.
9 S. Yokoyama, S. Mashiko, H. Kikuchi, K. Uchida and T. Nagamura, *Adv. Mater.*, 2006, **18**, 48.
10 I. C. Khoo, *Prog. Quantum Electron.*, 2014, **38**, 77.
11 H. Kikuchi, M. Yokota, Y. Hisakado, H. Yang and T. Kajiyama, *Nat. Mater.*, 2002, **1**, 64.
12 H. J. Coles and M. N. Pivnenko, *Nature*, 2005, **436**, 997–1000.
13 T.-H. Lin, C.-W. Chen and Q. Li, Self-Organized 3D Photonic Superstructure: Blue Phase Liquid Crystal*Anisotropic*

 This journal is © The Royal Society of Chemistry 2015

Open Access Article. Published on 17 September 2015. Downloaded on 12/10/2025 12:34:07 AM.
This article is licensed under a Creative Commons Attribution-NonCommercial 3.0 Unported Licence.

Nanomaterials: Preparation, Properties, and Applications, Springer International Publishing, 2015.
14 D. Xu, J. Yan, J. Yuan, F. Peng, Y. Chen and S. T. Wu, *Appl. Phys. Lett.*, 2014, **105**, 011119.
15 Y. Liu, Y. Li and S. T. Wu, *Appl. Opt.*, 2013, **52**, 3216–3220.
16 J.-M. Wong, J.-Y. Hwang and L.-C. Chien, *Soft Matter*, 2011, **7**, 7956–7959.
17 S. Hur, *et al.*, *Adv. Mater.*, 2013, **25**, 3002–3006.
18 L. Tian, *et al.*, *Liq. Cryst.*, 2013, **40**, 1446–1454.
19 H. Yoshida, Y. Tanaka, K. Kawamoto, H. Kubo, T. Tsuda, A. Fujii, S. Kuwabata, H. Kikuchi and M. Ozaki, *Appl. Phys. Express*, 2009, **2**, 121501.
20 M. Ravnik, G. P. Alexander, J. M. Yeomans and S. Zumer, *Proc. Natl. Acad. Sci. U. S. A.*, 2011, **108**, 5188.
21 L.-C. Chien, J. Y. Hwang and J.-M. Wong, *Blue phase liquid crystal nanocomposites and devices containing the same, US Pat.*, 8580144, 2013.
22 D. Xu, F. Peng and S. T. Wu, Polymer-Stabilized Blue Phase Liquid Crystals, *Handbook of Visual Display Technology*, 2nd edn, 2015.
23 F. Castles, *et al.*, *Nat. Mater.*, 2014, **13**, 817–821.
24 F. Castles, *et al.*, *Nat. Mater.*, 2012, **11**, 599.
25 J. Xiang and O. D. Lavrentovich, *Appl. Phys. Lett.*, 2013, **103**, 051112.
26 H. Kikuchi, S. Izena, H. Higuchi, Y. Okumura and K. Higashiguchi, *Soft Matter*, 2015, **11**, 4572.
27 J. Fukuda, *Phys. Rev. E: Stat., Nonlinear, Soft Matter Phys.*, 2010, **82**, 061702; J. Fukuda, *Phys. Rev. E: Stat., Nonlinear, Soft Matter Phys.*, 2012, **86**, 041704.
28 P. G. de Gennes and J. Prost, *The Physics of Liquid Crystals*, Oxford University Press, Oxford, 2nd edn, 1993.
29 G. Alexander and J. Yeomans, *Phys. Rev. E: Stat., Nonlinear, Soft Matter Phys.*, 2006, **74**, 061706.
30 M. Ravnik, G. P. Alexander, J. M. Yeomans and S. Zumer, *Faraday Discuss.*, 2010, **144**, 159.
31 J. Fournier and P. Galatola, *Europhys. Lett.*, 2005, **72**, 403.
32 M. Ravnik and S. Zumer, *Liq. Cryst.*, 2009, **36**, 1201.
33 K. V. Le, S. Aya, Y. Sasaki, H. Choi, F. Araoka, K. Ema, J. Mieczkowski, A. Jakli, K. Ishikawa and H. Takezoe, *J. Mater. Chem.*, 2011, **21**, 2855.
34 M. Lee, S. Hur, H. Higuchi, K. Song, S. Choi and H. Kikuchi, *J. Mater. Chem.*, 2010, **20**, 5813.
35 S. Kralj, S. Zumer and D. W. Allender, *Phys. Rev. A: At., Mol., Opt. Phys.*, 1991, **43**, 2943.
36 A. Martinez, *et al.*, *Nat. Mater.*, 2014, **13**, 258–263.
37 G. Mirri, M. Skarabot and I. Musevic, *Soft Matter*, 2015, **11**, 3347–3353.
38 Y. Xia, F. Serra, R. D. Kamien, K. J. Stebe and S. Yang, *Direct mapping of local director field of nematic liquid crystals*, 2015, submitted.
39 G. P. Alexander, B. G. Chen, E. A. Matsumoto and R. D. Kamien, *Rev. Mod. Phys.*, 2012, **84**, 497.
40 Y. Hisakado, *et al.*, *Adv. Mater.*, 2005, **17**, 96.
41 L. Rao, *et al.*, *Appl. Phys. Lett.*, 2011, **98**, 081109.
42 H. Tone, H. Yoshida, S. Yabu, M. Ozaki and H. Kikuchi, *Phys. Rev. E: Stat., Nonlinear, Soft Matter Phys.*, 2014, **89**, 012506.